Post-Print

This is the accepted version of:

F. Salucci, L. Trainelli, C.E.D. Riboldi, A. Rolando
Sizing of Airport Recharging Infrastructures in Support to a Hybrid-Electric Fleet
in: AIAA Scitech 2021 Forum, AIAA, 2021, ISBN: 9781624106095, p. 1-14, AIAA 2021-1682
[AIAA Scitech 2021 Forum, Virtual Event, Jan. 11-15, 19-21, 2021]
doi:10.2514/6.2021-1682

Sizing of Airport Recharging Infrastructures in Support to a Hybrid-Electric Fleet

Francesco Salucci*, Lorenzo Trainelli†, Carlo E.D. Riboldi‡ and Alberto Rolando§
Politecnico di Milano, Milano, 20156, Italy

Introducing airplanes which are powered, totally or partially, by electricity, poses significant challenges for the on-ground operations at the airports and possibly for the flight scheduling as well. Airport operators will need to accommodate an overall new network of electric cables, battery swapping stations and/or plug-in chargers. Furthermore, battery charging is expected to take longer than conventional refueling, prolonging the turnaround time of an aircraft. The ARES (Airport Recharging Equipment Sizing) methodology is proposed to evaluate the needed infrastructure and derive the best possible battery charging program, on the basis of the characteristics of the aircraft, the airport flight scheduling, and the electricity and equipment pricing. The method is applied to realistic case studies, providing results that optimize the infrastructural and operational costs while preserving the current flight scheduling in a large European airport.

I. Introduction

In order to totally unfold the potential of Pure-Electric (PE) and Hybrid-Electric (HE) propulsion, globally reducing the emission of chemical pollutants without negatively impacting normal air transport operations, it is necessary to cope with the technical needs of these novel power-train types at a system level. In particular, since such power-trains heavily rely on batteries [1–3], possibly even when intimately integrated in the airframe structure [4], the management of these energy storage systems and the impact on airport operations need to be accurately planned. From the viewpoint of larger airport managers, as well as for most flight schools operating both an airfield and a General Aviation (GA) fleet, sizing the battery management infrastructure is clearly a major concern, bound to significant reconfiguration costs. These can be quantified only by an accurate and simultaneous analysis of the needs of a new technologically advanced fleet, of all components in the recharge infrastructure on ground, and of its interface with the electric grid of the airport.

The present research introduces a novel method to model and optimally size a ground battery recharging system. Two major recharge options are considered: Battery Swapping Stations (BSSs) and Battery Plugin Chargers (BPCs). BSSs can be employed if the aircraft batteries can be loaded and unloaded from the aircraft before or after a flight, while BPCs are capable of recharging the batteries without removing them from the aircraft. Compared to BPCs, BSSs allow a lower turnaround time for the aircraft, provided fully-charged spare batteries are available to be embarked in the departing aircraft. Operating a BPC is conceptually similar to refilling a tank for a conventionally-powered aircraft. However, due to the technological limits of batteries and of their recharging process, nowadays the recharging time may prove unbearable for larger aircraft, making BSS more fitting for airports supporting an important regional traffic. Conversely, as far as smaller aircraft are concerned, like in the GAs segment, the relative advantage of these systems in the complete infrastructure is not known *a priori*.

A further element which needs to be accurately modeled is the varying price of the electric energy supply. This usually evolves periodically over time, with peaks during working days and minima at night or in the weekends, with both energy and peak power requested contributing to the total daily cost. Thanks to the features of current electric grids, which are ready for unpredictable input from renewable sources such as wind and solar power-plants, and to the expected availability of large numbers of batteries on ground, the chance to supply energy from the batteries to the grid is considered, as a potential "negative cost" for the airport or fleet manager.

After introducing the models of the ground infrastructure elements, an optimal approach is introduced providing the sizing to the needs of a given fleet. Quantities to be determined include the number of BSSs and/or BPCs and the number of spare batteries (in the case of using BSSs), whereas the merit function of the optimization includes both

*PhD candidate, Department of Aerospace Science and Technology. AIAA Student Member
†Associate Professor, Department of Aerospace Science and Technology. AIAA Member
‡Assistant Professor, Department of Aerospace Science and Technology. AIAA Member
§Adjunct Professor, Department of Aerospace Science and Technology.

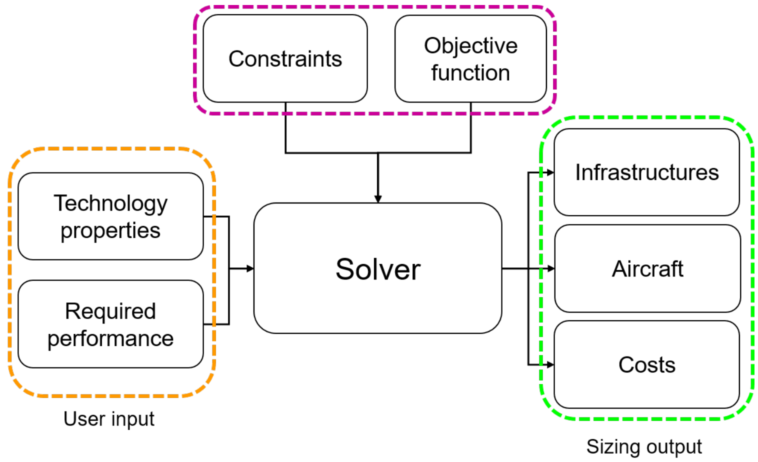

Fig. 1 Schematic of the optimization process.

operating and procurement costs. The former are related to energy supply, while the latter depend on the considered subsystems and take into account life cycle costs. In addition, the optimization provides the optimal scheduling of the recharging procedures based on the fleet operations and turnaround times. This methodology has been implemented in the Airport Recharging Equipment Sizing (ARES) tool and applied to a number of study cases ranging from smaller local GA aerodromes to large airports. As an example, the application of ARES to the reconfiguration of the Athens International airport airport in support to a future regional HE fleet is considered here.

This work is part of a larger effort aimed at providing scenario predictions for the future implementation of a radically new regional air transportation system. This concept is included in the scope of the EU-funded MAHEPA (Modular Approach to Hybrid Electric Propulsion Architecture) and UNIFIER19 (Community Friendly Miniliner) projects, in which research activities are carried out towards the scalability of HE technologies from smaller GA aircraft to passenger and freight air transport vehicles in the FAR Part 23/CS-23 certification category, and possibly in the larger FAR Part 25/CS-25. Elements of this scenario are presented in [5, 6], where novel methodologies for the prediction of the potential traveling demand for short-haul air transportation are discussed, and [3, 7], where a new approach to the prediction of acoustic emission by HE aircraft operations in the vicinity of an airport is offered.

II. Optimal sizing

The ARES sizing framework consists of an optimization process trough which infrastructural costs and operational expenses are minimized. The sizing of the recharging equipment is driven by the fleet type composition, which involves the properties of aircraft, batteries, and chargers, and by the flight scheduling at the airport. The goal is to design an infrastructure that can satisfy the charging requests, while minimizing the investment and operational costs of the recharging facility through a Mixed Integer Linear Programming (MILP) optimization. The general concept is sketched in Figure 1.

A. Cost Function

The aim of the optimization is to select the solution with the lower total cost. Thus, the objective function J to be minimized contains a collection of cost items (Figure 2, right), as

$$J = \underbrace{C_E + C_P}_{\text{electricity cost}} + \overbrace{C_{BSS} + C_{BPC}}^{\text{chargers cost}} + \underbrace{C_B}_{\text{batteries cost}} \tag{1}$$

The cost of energy C_E is related to the energy amount E_t^p absorbed from the grid over a given time step ΔT, and to the monetary value per energy unit λ_t:

$$C_E = \sum_{t=0}^{T} \lambda_t E_t^p, \tag{2}$$

Clearly, the value calculated in Eq. 2 is a function of the time frame T considered for the analysis. That value should be taken consistently with the definitions of the other components of J, as described through the next equations.

The cost of power can be expressed as

$$C_P = \frac{E_t^p}{\Delta t} c_P \frac{N_D}{30}, \tag{3}$$

where the c_P term represents the cost per unit peak-power per month, and the value of $\left(\frac{N_D}{30}\right)$ the number of days N_D in the considered analysis in a month. The value of N_D implicitly defines the limit for the sum in Eq. 2.

The components C_{BSS} and C_{BPC} represent the procurement cost of the BSS and the BPC respectively. They can be written as

$$C_{BSS} = N_{BSS}\, c_{BSS} \frac{N_D}{T_{BSS}}, \tag{4}$$

$$C_{BPC} = N_{BPC}\, c_{BPC} \frac{N_D}{T_{BPC}}, \tag{5}$$

where N_{BSS}, c_{BSS}, N_{BPC} and c_{BPC} are the number and acquisition cost per unit of BSS and BPC respectively, and T_{BSS} and T_{BPC} are the expected lifespan of the devices.The cost per unit c_{BSS} and c_{BPC} can be defined based on a technological regression, as a function of the charging power [8]. For example, for the BSS it can be expressed in Euro as

$$c_{BSS} = (14\,601 \cdot \ln P_{BSS} - 19\,968)\,(1 + \chi)\,, \tag{6}$$

where the term $\chi = 10\%$ has been added to take into account maintenance costs.

Lastly, the cost model for batteries yields

$$C_B = N_B c_B \frac{N_D}{T_B} \tag{7}$$

where c_B is the acquisition cost per unit battery and T_B the expected lifespan of the device.

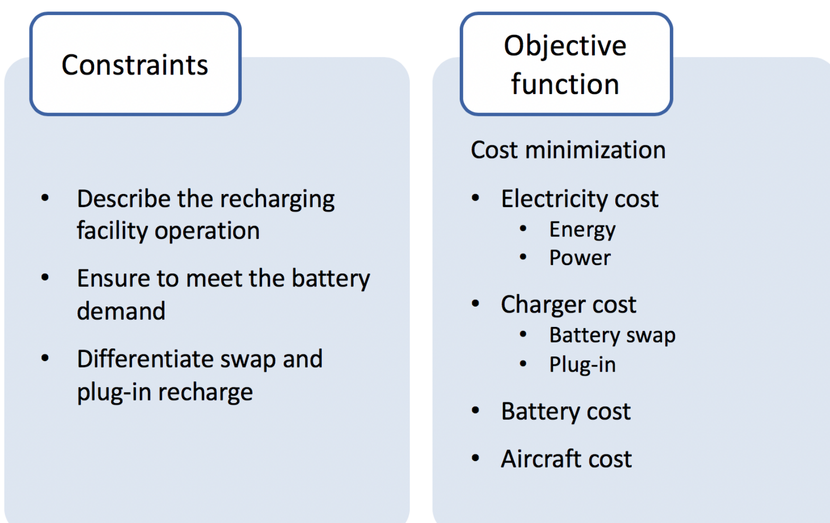

Fig. 2 Objective function and constraints.

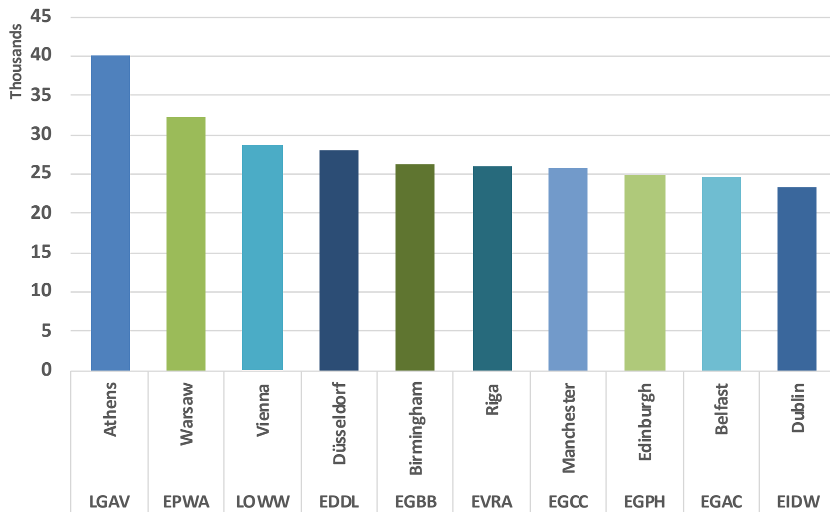

Fig. 3 Airport ranking for number of regional aircraft movements in Europe in 2019.

B. Constraints

Constraints are then added to trigger the optimization process: they oversee the physics and the coherence of the system, considering limits on the State Of Charge (SOC) of each battery at every time step and on maximum charging/discharging power, and take into account the flight departure schedule (Figure 2, left).

In order to consider both BSSs and BPCs, penalties are added:

- when a battery is charged in the BSS, it is unavailable for the time needed to perform the swap; during this time, the battery cannot be charged, nor be used to fly.
- when a BPC is used, it requires the aircraft to stay on ground to perform the recharge.

A detailed presentation of the ARES formulation, including all imposed constraints, is given in [9, 10].

III. Study case

A. Airport selection

The procedure described in Section II was applied to the determination of the infrastructure requirements for managing PE and HE aircraft fleets at Athens International Airport Eleftherios Venizelos (ICAO code: LGAV). This has been selected for this study since it was the European airport with the largest number of propeller-driven regional aircraft movements in the years 2015–2019 [11].

Figure 3 shows the European ranking on 2019 regional turboprop aircraft movements (commercial air flights: passengers, freight and mail) considering the models being currently operated: ATR72, ATR42 and DASH 8. No inter-continental hubs appear in the chart, whereas five airports (Birmingham/EGBB, Manchester/EGCC, Edinburgh/EGPH, Belfast/EGAC, and Dublin/EIDW) are located in either UK or Ireland, hinting to the convenience of using regional turboprop aircraft to connect insular regions. Indeed, regional aircraft are widely used to connect the numerous Greek islands between them and to the mainland, thus Athens/LGAV airport makes a good test case to assess the infrastructural needs of massive regional aircraft operations.

B. Hybrid-electric aircraft battery needs

In compliance to the current operational scenario at Athens/LGAV, three regional airplanes were considered for the present case study:

1) Bombardier Dash 8 Q400 (78 passengers),
2) ATR42 (48 passengers),
3) ATR72 (70 passengers).

This is the class of aircraft that could most likely see, in a short term, the introduction of versions designed to include

Table 1 Aircraft characteristics and battery prices.

Name	Pax	Battery Price [k€]	Battery capacity [kWh]
HE-DH8	78	253.4	1,400
HE-ATR42	48	184.8	1,000
HE-ATR72	70	237.6	1,300

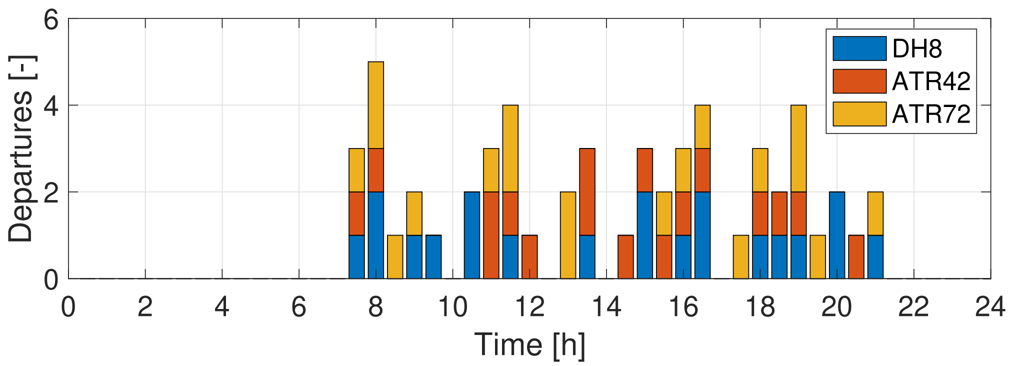

Fig. 4 Departures from LGAV used for the study case.

an HE power-train, and will therefore include a battery. We assumed to replace the current conventionally-powered fleet with new vehicles featuring a serial HE power-train. This includes the definition of a specialized mission profile where taxiing out, taking off and climbing out to a defined HE transition altitude (here set to 3,000 ft) is performed in a zero-emission PE mode. Subsequently, the fuel-burning Power Generation System (PGS) is be turned on, for providing energy during final climb and cruise phase, as well as for recharging the batteries, if needed. Finally, when descending below the HE transition altitude, the PGS is shut off, so final descent, approach, landing and taxi-in will again be performed in PE mode. This strategy allows to drastically reduce chemical and noise emissions in the vicinity of the airport and related overflown communities.

The technical specifications of the electrified airplanes, were obtained by means of the HYPERION preliminary sizing tool [12, 13], an element of a suite of recently-developed procedures dedicated to PE and HE aircraft design. For the sake of clarity, the serial HE versions designed through HYPERION are named as the original model adding an "HE-" prefix, yielding the HE-DH8, HE-ATR42 and HE-ATR72, respectively.

Table 1 shows the estimated battery capacity and cost for each of the aforementioned models. In this study case, the flights taking off from LGAV on Friday, December 13, 2019 (a peak-traffic period) were used to build up the flight schedule fed to the optimization algorithm. The fleet operating at that time was composed by nine ATR 42, seven ATR 72 and ten Bombardier Dash 8 Q400. The bar plots in Figure 4 and Table 2 depict the relevant departures for the study case, gathered from public flight tracking services [14]. A budgetary price for the batteries (including cells and battery pack) was calculated using 2018 Lithium-ion battery price, i.e. approximately 176 €/kWh [15].

Table 2 Summary of the flight schedule from LGAV used for the study case.

	# a/c	**# departures**	**max departures/h**
DH8	10	20	3
ATR42	9	16	4
ATR72	7	19	3
Total	26	55	8

Table 3 Properties and costs of chargers employed in the study case.

Parameter	Value
250 kW chargers	66.7 k€
1000 kW chargers	89.0 k€
Charger life	10 years
Charging efficiency	93%

C. Charging equipment

Chargers cost, recharge process efficiency, charger life and other data can be found in Table 3. Two different values of the recharge power P_{BSS}, P_{BPC} of the ground recharging devices have been selected: 250 kW and 1,000 kW. These are representative of current automotive charging infrastructure: 250kW is already available for Tesla customers who can use Tesla Superchargers v3 [16], while 1,000 kW are currently under advanced development to be employed to recharge full-electric trucks (such as the Tesla MEGACharger [17]).

D. Electricity pricing

Three pricing schemes were applied to the simulations for what concerns the cost of electricity λ_t:

1) **Scheme A**: electric energy costs more during the day and less during the night;
2) **Scheme B**: electric energy costs less during the day and more during the night;
3) **Scheme C**: constant price of electricity throughout the 24 hours.

Scheme A is representative of the current way electric energy is priced. In particular, there is a higher daytime energy charge (from 07:00 to 23:00) and a lower night-time energy charge (from 23:00 to 07:00). An example is given by the electricity prices in Greece for the year 2018 as reported in Table 4.

Scheme B and Scheme C are inspired from assumptions on future electricity pricing. In particular, electricity rates depend on multiple variables, such as electricity generating prices, government taxation or incentives, local weather conditions, transmission and distribution networks, and multi-tiered market control. Depending on the consumer base, the price or rates may also vary, usually by residential, commercial and industrial connections. The sources of energy that are commonly used for electricity production are fossil fuels, nuclear energy, and renewable energy sources. The majority of today's electric energy is produced using fossil fuels and nuclear energy. This type of production happens in big power stations running 24/7 in a continuous way. Since electricity generation is more or less constant, its price is determined by the demand curve: i.e. electricity costs more during working hours. However, the use of wind and solar energy will determine an irregular electricity generation pattern. Thinking of solar, the availability will be higher during the day and almost zero during the night. Moreover, both solar and wind energy can be heavily influenced by weather conditions. However, the most import factor that influences the electricity price is the balance between the demanded power and the available power being produced [18]. Hence the end-user cost of electricity actually depends on the supply and demand economic model.

Because of the unpredictable availability of renewable energy sources, energy is usually captured for use at a later time. For instance, solar farms are often fitted with batteries to meet grid output control requirements while offshore

Table 4 Electricity charges applied to Scheme A.

Energy charge - λ_t		
0.0648	€/kWh	Daytime
0.0777		Nighttime
Power charge - c_P		
10.508	€/kW/month	Daytime
2.508		Nighttime

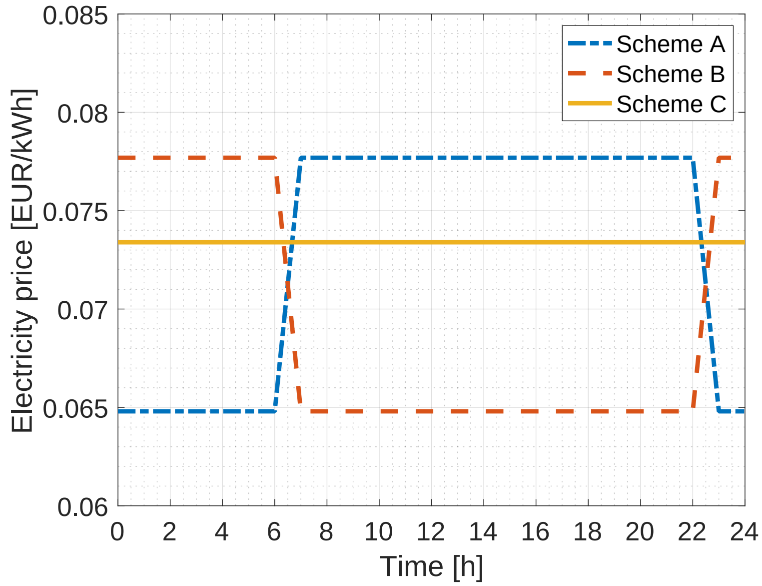

Fig. 5 Price of electricity during the 24 hours for Schemes A, B and C.

wind farms can feature electrolyzers to produce hydrogen from sea water using electricity provided by wind turbines. However, storing electricity has its costs and immediate usage is preferred. For these reasons, the usual day/night pricing scheme could disappear in the future (about 2040), when electricity will be mostly generated with renewable energy sources [19]. To represent this scenario, electricity pricing Scheme B was introduced in the study case supposing solar energy is the main generating source. In such case, electric energy is mainly produced during the day, leading to a lower cost if used in those hours. Scheme C is representative of an intermediate scenario (2030), where electricity is produced with a balanced mixture of renewable and non-renewable sources.

Figure 5 shows the value assumed by the electric energy price per kWh λ_t of Scheme A, B and C. The cost of power per kW c_P was also taken equal to that of Scheme A but inverting night and day (Scheme B) or using the mean value (Scheme C)

IV. Results

A. Using 250 kW chargers

The electric energy consumption using 250 kW chargers is displayed in Figure 6 for the three different electricity pricing schemes. Blue bars represent electric energy absorbed every 30 minutes. The orange line delineates the variation of λ_t during the day. It is apparent that with Scheme A a greater amount of electricity is uniformly drained from the grid during the night. On the other hand, energy consumption decreases during the day, but still responds to the increasing battery demand. Quite the contrary happens with Scheme B: electric energy consumption peaks during the day, while lying low during the night, only to guarantee a minimum charge level of the batteries. This bipolar behavior clearly disappears with a constant electricity pricing, i.e. Scheme C, where the energy consumption is more or less constant throughout the 24 hours and basically mimics the battery demand from the flight schedule.

Battery charging can either be carried out by a BSS or a BPC and ARES can be set free to choose the optimal mix. In all the cases shown here, since the fleet of aircraft is fixed, a mixed usage of BSS and BPC comes out from the simulation. This is apparent in the results summarized in Table 5. It is interesting to note that charging a battery takes between 4.0 and 5.6 hours, depending on the aircraft, when charged at full power. This recharging time is not compatible with the available fleet of aircraft and could negatively impact on the flight schedule. Therefore, BSS charging is employed to recharge some batteries while these are disembarked from the airplane. As a result, seven BSSs are employed together with ten BPCs for Scheme A. Scheme B uses more chargers: 10 BSSs and 9 BPCs. The reason might be that charging the batteries during the day, while the departures are happening, leads to a higher need for chargers, as the same number of batteries is used by Scheme B and Scheme A. Chargers are in fact less expensive than

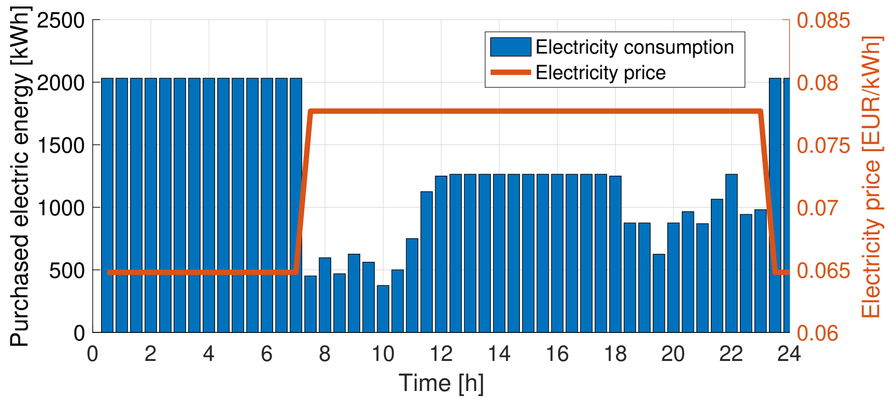

(a) Scheme A

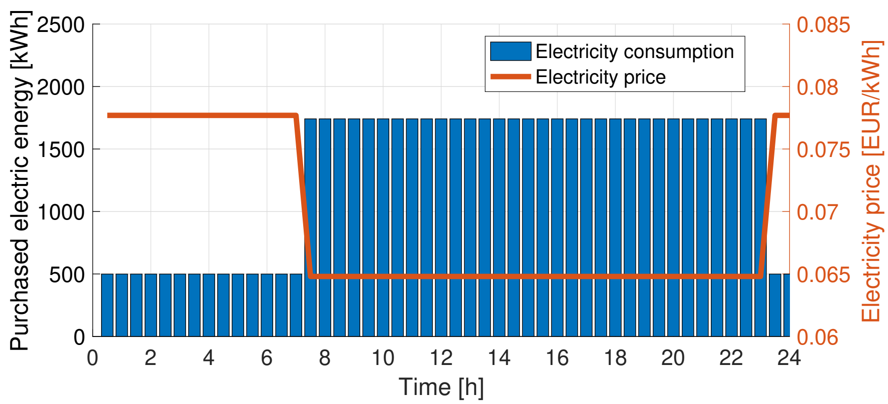

(b) Scheme B

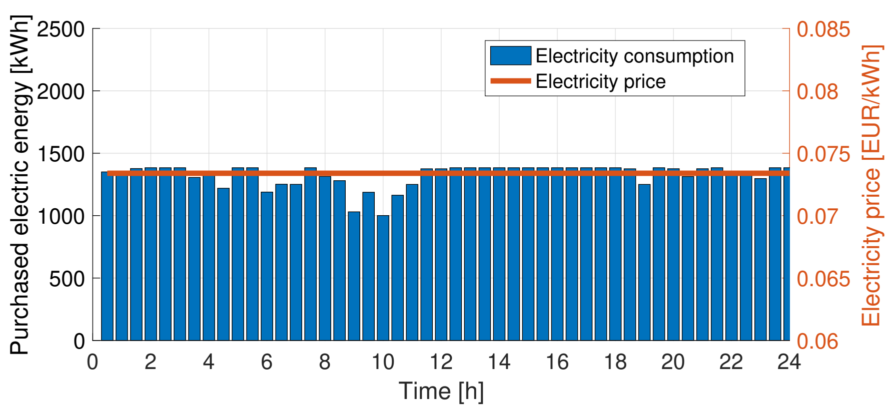

(c) Scheme C

Fig. 6 Energy consumption at LGAV with 250 kW chargers.

Table 5 LGAV sizing results with 250 kW chargers.

Item	Unit	Scheme A	Scheme B	Scheme C
No. airplanes (HE-DH8+HE-ATR42+HE-ATR72)	-	10+9+7		
No. charges	-	20+17+19	20+17+19	20+17+19
Energy consumption	kWh	63,704	63,704	63,704
No. batteries	-	38 (13+12+13)	38 (13+12+13)	37 (13+12+12)
No.BSSs	-	7	10	6
No. BPCs	-	10	9	11
Peak power	kW	4,063	3,482	2,767
Electricity cost	k€	4,530	4,231	4,676
Power cost	k€	340	291	601
Battery life	years	1.49	1.49	1.45

additional spare batteries. Scheme C lies in the middles with the same total number of chargers as Scheme A but with one extra BPC (6 BSSs and 11 BPCs).

The biggest saving in the cost of electricity is achieved by Scheme B: 16 hours of cheap rate during the day, versus 8 hours of expensive rate during the night. In addition, the greater availability of chargers helps keeping eme B peak power lower than Scheme A (-0.58 MW). However, the winner for the lowest peak power is Scheme C, (-21% with respect to Scheme B and -32% with respect to Scheme A). This cannot optimize the electricity cost, so it plays for minimizing the peak power, but still has to trade one battery to save on the total, while the number of spare batteries used by Scheme A and B are the same.

The full recharging schedule can be observed in Figure 7, where the grids represent the SOC of each battery at every time step t. Small green squares indicate when the battery is charging with a BSS, while small blue squares are used for BPCs. Small white squares mean that the battery is not under charge or that the SOC is zero.

B. Using 1,000 kW chargers

Boosting the charging power to 1,000 kW brings clear advantages both in the number of batteries and chargers needed and in the total cost of electricity. Table 6 shows that the number of chargers plummets from 17-19 in the 250 kW cases to 7-8 in the 1 MW case: Scheme A features three BSSs and five BPCs, Scheme B two BSSs and five BPCs, and Scheme C three BSSs and five BPCs. Also, the total number of batteries is way lower: 24 (8 for each type of airplane) down from 37-38 in the 250 kW case.

Figure 8 depicts the absorbed electric energy in the 1,000 kW charger cases. With Scheme A, no recharges occur between 07:30-10:30 and from 20:00-23:00 avoiding to buy electricity when it is more expensive. On the other hand, Scheme B electricity is bought only during the day, because it is cheaper. Scheme C, instead, shows a mixed behavior: electric energy is mostly used when the battery demand is higher and simply stops when the batteries are all charged.

Figure 9 shows the grids with the overall charging schedule, making immediately clear that charging one battery takes around 4 times less than the 250 kW case. This helps keeping down the peak power, by distributing the recharges in an efficient way.

V. Conclusion

The Airport Recharging Equipment Sizing (ARES) tool was applied to determine optimal sizing and scheduling solutions for the battery recharging infrastructure of a major airport home to a sizeable regional turboprop traffic, Athens International Airport (LGAV), assuming to replace the current fleet of ATR 42, ATR72 and DASH 8 with corresponding serial HE models. ARES minimizes the cost of consumed electric energy as well as acquisition costs for battery recharging devices and batteries, satisfying a pre-determined flight schedule. The flight schedule employed for the present application was taken from actual flight data. Two types of chargers have been considered: Battery Plug-In Chargers and Battery Swapping Stations. Charging power was set according to current and future values typically found in automotive applications: 250 and 1000 kW. Three different scenarios for electricity pricing were envisioned: one

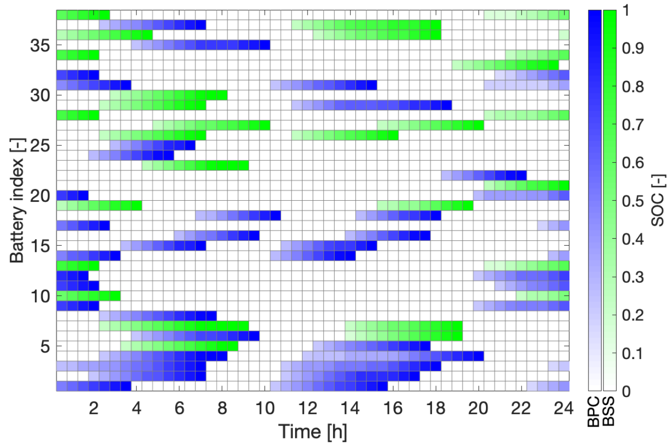

(a) Scheme A

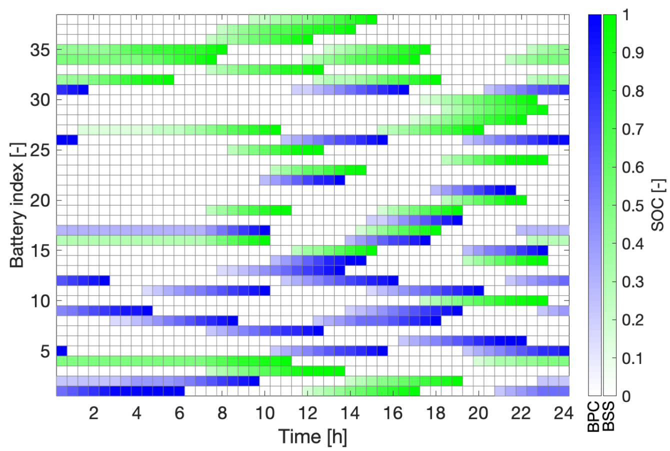

(b) Scheme B

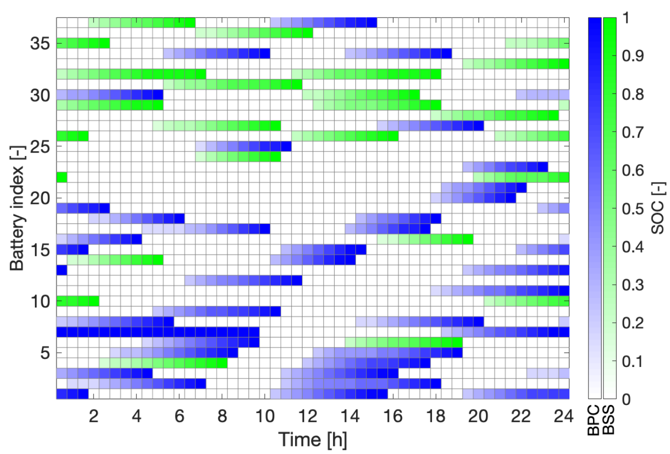

(c) Scheme C

Fig. 7 Battery state of charge and charging schedule at LGAV using 250 kW chargers.

corresponding to the current day/night rates (Scheme A), a futuristic one favoring the use of renewable solar energy during the day (Scheme B) and a mixed one with a constant energy and power rate (Scheme C).

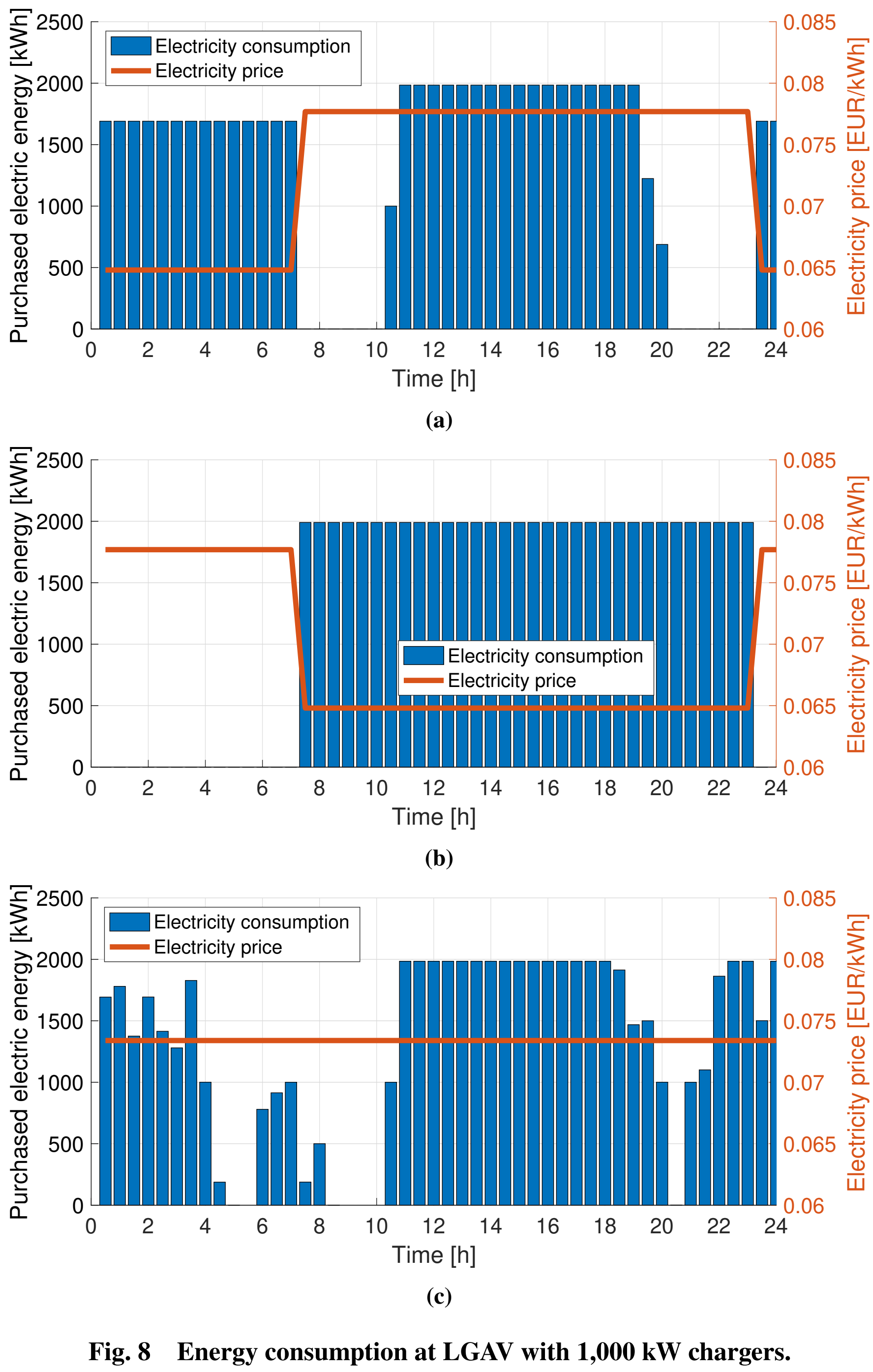

Fig. 8 Energy consumption at LGAV with 1,000 kW chargers.

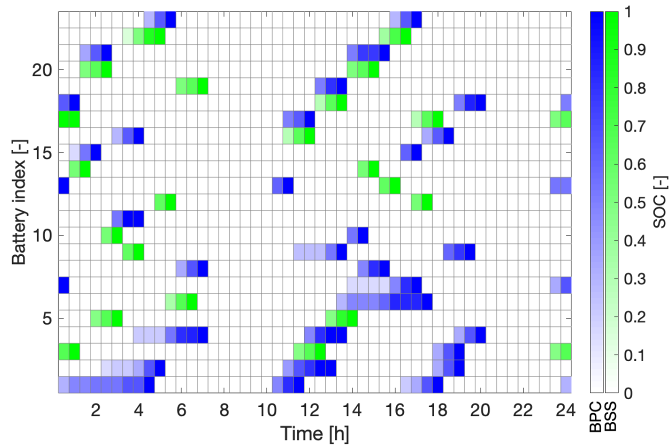

(a) Scheme A

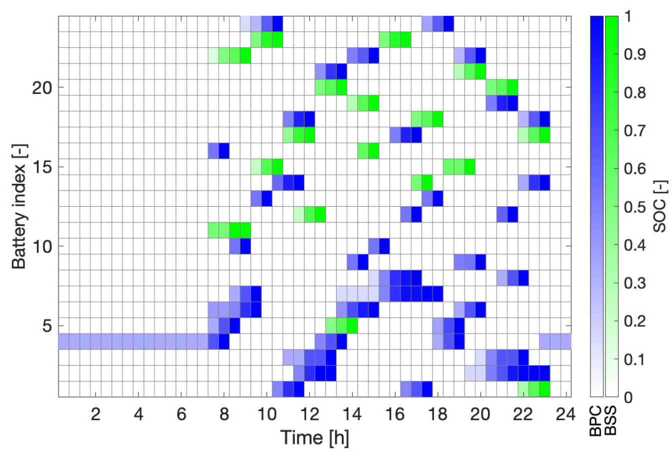

(b) Scheme B

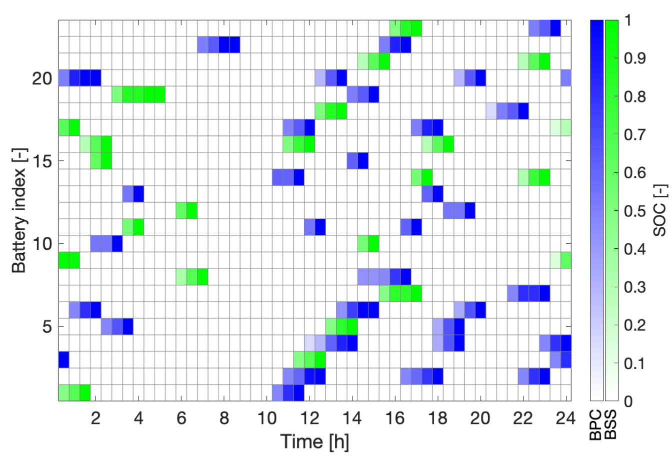

(c) Scheme C

Fig. 9 Battery state of charge and charging schedule at LGAV using 1,000 kW chargers.

Table 6 LGAV sizing results with 1,000 kW chargers.

Item	Unit	Scheme A	Scheme B	Scheme C
No. airplanes (HE-DH8+HE-ATR42+HE-ATR72)	-	10+9+7		
No charges	-	20+17+19	20+17+19	20+17+19
Energy consumption	kWh	63,704	63,704	63,704
No. batteries	-	24 (8+8+8)	24 (8+8+8)	24 (8+8+8)
No. BSS	-	3	2	3
No. BPC	-	5	5	5
Peak power	kW	3,969	3,969	3,969
Electricity cost	€	4,601	4,128	4,676
Power cost	€	332	332	861
Battery life	years	0.94	0.94	0.94

Results show that whenever the charging power is limited, i.e. in the 250 kW case, recharging times get too long, leading to a large number of required spare batteries and chargers. On the other hand, a higher charging power can help in reducing the equipment costs (less spare batteries, less chargers), but lead to a higher electric energy cost. Also, Scheme B seems to be the best for the cheapest electricity pricing schemes. Within Scheme B, in fact, there is more space to look for an optimal recharging schedule, and hence to reduce the operational costs, performing better in the 1,000 kW than in the 250 kW one. However, the situation is not drastically different from Scheme A, while Scheme C, where electricity rates are constant in time, appears as the most expensive one with small room for optimization. To summarize, higher charging power is the factor that will help the most in reducing turnaround time and ease airport operations. However, high power might also impact on battery life, a factor which has not been included in the presented case study. Future applications of ARES shall include this effect, for increased reliability of the sizing solution.

Acknowledgments
The research leading to the presented results has received funding from Project MAHEPA, financed by the EU H2020 Programme under Grant Agreement N. 723368.

References
[1] Misra, A., "Energy Storage for Electrified Aircraft: The Need for Better Batteries, Fuel Cells, and Supercapacitors," *IEEE Electrification Magazine*, Vol. 6, No. 3, 2018, pp. 54–61. https://doi.org/10.1109/MELE.2018.2849922, URL https://ieeexplore.ieee.org/document/8456876/.

[2] Riboldi, C. E., Gualdoni, F., and Trainelli, L., "Preliminary weight sizing of light pure-electric and hybrid-electric aircraft," *Transportation Research Procedia*, Vol. 29, 2018, pp. 376 – 389. https://doi.org/https://doi.org/10.1016/j.trpro.2018.02.034, URL http://www.sciencedirect.com/science/article/pii/S2352146518300383, aerospace Europe CEAS 2017 Conference.

[3] Riboldi, C. E. D., Trainelli, L., Mariani, L., Rolando, A., and Salucci, F., "Predicting the effect of electric and hybrid-electric aviation on acoustic pollution," *Noise Mapping*, Vol. 7, No. 1, 2020, pp. 35–56. https://doi.org/10.1515/noise-2020-0004, URL https://www.degruyter.com/view/journals/noise/7/1/article-p35.xml, publisher: De Gruyter Section: Noise Mapping.

[4] Riboldi, C. E. D., Trainelli, L., and Biondani, F., "Structural Batteries in Aviation: A Preliminary Sizing Methodology," *Journal of Aerospace Engineering*, Vol. 33, No. 4, 2020, p. 04020031. https://doi.org/10.1061/(ASCE)AS.1943-5525.0001144, URL https://ascelibrary.org/doi/abs/10.1061/%28ASCE%29AS.1943-5525.0001144, publisher: American Society of Civil Engineers.

[5] Trainelli, L., Riboldi, C. E. D., Rolando, A., and Salucci, F., "Methodologies for the Initial Design Studies of an Innovative Community-Friendly Miniliner," *IOP Conference Series: Materials Science and Engineering*, 2021. Accepted.

[6] Salucci, F., Trainelli, L., Bruglieri, M., Riboldi, C. E. D., and Rolando, A., "Capturing the Demand for an Electric-Powered Short-Haul Air Transportation Network," *AIAA SciTech 2021 Forum*, January 11–15,2021.

[7] Salucci, F., Riboldi, C. E. D., Trainelli, L., Rolando, A., and Mariani, L., "A Noise Estimation Procedure for Electric and Hybrid-Electric Aircraft," *AIAA SciTech 2021 Forum*, January 11–15,2021.

[8] Schroeder, A., and Traber, T., "The economics of fast charging infrastructure for electric vehicles," *Energy Policy*, Vol. 43, 2012, pp. 136 – 144. https://doi.org/https://doi.org/10.1016/j.enpol.2011.12.041, URL http://www.sciencedirect.com/science/article/pii/S0301421511010470.

[9] Salucci, F., Trainelli, L., Faranda, R., and Longo, M., "An optimization Model for Airport Infrastructures in Support to Electric Aircraft," *2019 IEEE Milan PowerTech*, Milan, Italy, June 2019, pp. 1–5. https://doi.org/10.1109/PTC.2019.8810713.

[10] Trainelli, L., Salucci, F., Riboldi, C. E. D., and Rolando, A., "Optimal Sizing and Scheduling of Airport Recharging Infrastructures in Support to Electric Fleets," 2021. Submitted for publication.

[11] "Airport traffic data by reporting airport and airlines - Eurostat," , 2020. URL https://ec.europa.eu/eurostat/web/products-datasets/-/avia_tf_apal.

[12] Trainelli, L., Salucci, F., Rossi, N., Riboldi, C. E. D., and Rolando, A., "Preliminary Sizing and Energy Management of Serial Hybrid-Electric Airplanes," *XXV Congresso Nazionale AIDAA*, Roma, Italy, September 9–12,2019.

[13] Trainelli, L., Riboldi, C. E., Salucci, F., and Rolando, A., "A General Preliminary Sizing Procedure for Pure-Electric and Hybrid-Electric Airplanes," *1st Aerospace Europe Conference (AEC 2020)*, Bordeaux, France, February 25–28, 2020, pp. 1–10.

[14] Flightradar24, "Live Flight Tracker - Real-Time Flight Tracker Map," , 2019. URL https://www.flightradar24.com/data/airports/ath, library Catalog: www.flightradar24.com.

[15] "A Behind the Scenes Take on Lithium-ion Battery Prices," , Mar. 2019. URL https://about.bnef.com/blog/behind-scenes-take-lithium-ion-battery-prices/, library Catalog: about.bnef.com Section: Report.

[16] "Supercharger | Tesla," , 2019. URL https://www.tesla.com/supercharger, library Catalog: www.tesla.com.

[17] "Tesla is working with mysterious third-parties to deploy Megacharger network for electric semi trucks - Electrek," , 2020. URL https://electrek.co/2020/10/22/tesla-mysterious-third-parties-megacharger-network-electric-semi-trucks/.

[18] "Historical data (until December 2015)," , 2020. URL https://www.entsoe.eu/data/data-portal/.

[19] "Electricity generation by fuel and scenario, 2018-2040 – Charts – Data & Statistics," , 2020. URL https://www.iea.org/data-and-statistics/charts/electricity-generation-by-fuel-and-scenario-2018-2040.